Dyes and Pigments 104 (2014) 75–82

Contents lists available at ScienceDirect

Dyes and Pigments

journal homepage: www.elsevier.com/locate/dyepig

Organic dyes incorporating a thiophene or furan moiety for efficient dye-sensitized solar cells

Jinxiang He[a], Jianli Hua[a], Guangxia Hu[b], Xi Jiang Yin[c], Hao Gong[b], Chunxiang Li[c,*]

[a] Key Laboratory for Advanced Materials, Institute of Fine Chemicals and Department of Chemistry, East China University of Science and Technology, 130 Meilong Road, Shanghai 200237, PR China
[b] Department of Materials Science and Engineering, National University of Singapore, 10 Kent Ridge Crescent, Singapore 119260, Singapore
[c] Advanced Materials Technology Centre, Singapore Polytechnic, 500 Dover Road, 139651, Singapore

ARTICLE INFO

Article history:
Received 19 June 2013
Received in revised form
16 December 2013
Accepted 24 December 2013
Available online 7 January 2014

Keywords:
Alkyl functionalized carbazole
Thiophene
Furan
Organic dye
Dye-sensitized solar cell
Photovoltaic

ABSTRACT

Four novel carbazole organic dyes containing either a furan or a thiophene unit as the conjugated bridge have been designed, synthesized and characterized for nanocrystalline TiO_2 dye-sensitized solar cells. The modified carbazole containing linear or branched alkyl side chain acts as an electron donor, triphenylamine acts as an electron-donating group and cyanoarylic acid acts as an electron acceptor and anchoring unit. The absorption spectra, electrochemical, photovoltaic and sensitizing properties of the new dyes were fully characterized. Among these four dyes, the dye incorporating an octyl-substituted carbazole and disubstituted furan shows the best photovoltaic performance: a maximum monochromatic incident photon-to-current conversion efficiency of 92.4%, a short-circuit photocurrent density of 13.26 mA cm^{-2}, an open-circuit photovoltage of 724 mV, and a fill factor of 0.66, corresponding to an overall conversion efficiency of 6.68% under standard global AM 1.5 solar light condition. The results indicate that the introduction of longer alkyl chain into the carbazole moiety will retard recombination and the introduction of furan as the conjugate bridge will increase the photocurrent response. For comparison, the ruthenium dye, designated as **N719**, sensitized TiO_2 solar cell showed an efficiency of 6.98% under the same experiment conditions.

1. Introduction

Increasing demand for energy consumption has led to a greater focus on renewable energy resources research all over the world over the past couple of decades. Dye-sensitized solar cells (DSSCs), considered as a promising alternative to conventional solar cells, have attracted intense attention due to the relatively high solar power-to-electricity conversion efficiency (η) and potentially low cost production since Grätzel and co-workers reported DSSCs high efficiency in 1991 [1]. The photosensitizer is one of the key materials in DSSCs, which plays an important role in determining the performance of the solar cells. Central to this device is a TiO_2 nanoparticle film that provides a large surface area for the adsorption of dye sensitizers, which absorbs light and injects electrons into the conduction band of the TiO_2 after light excitation and converts the sunlight to photocurrent. To date, Ru–polypyridine complexes have achieved power conversion efficiencies over 11% [2,3] under standard global air mass 1.5 solar simulated conditions and also show favorable stabilities [4]. However, their practical applications are restricted by the limited supply and high cost of ruthenium metal. In recent years, the interest in metal-free organic dyes as substitutes for noble metal complexes is increasing owing to their high molar extinction coefficient, simple synthesis, low cost and facile molecular design. An enormous number of studies have been focused on molecular engineering of chromophores to attain a capability of panchromatic light-harvesting [5]. A variety of organic dyes, such as diketopyrrolopyrrole dyes [6,7], phenothiazine [8–10], cyanine [11–14], merocyanine [15,16], coumarin Refs. [17–19], thiophene [20], indoline [21–26], hemicyanine [27–29], phenoxazine [30], carbazole [7,31–34] and fluorine based dyes [35–37] have been reported and found to exhibit promising device characteristics. Impressive photovoltaic performances have been obtained using organic dyes with efficiency exceeding 10% [38–40].

Organic dyes commonly consist of donor, linker, and acceptor groups (*i.e.*, a D–π–A molecular structure). Their various properties could be finely tuned by alternating independently or matching the different groups of D–π–A dyes [41–43]. Generally organic dyes used for efficient solar cells are required to possess broad and intense spectral absorption in the visible light region. One strategy

---

* Corresponding author. Tel.: +65 68708241; fax: +65 68708083.
E-mail address: licx@sp.edu.sg (C. Li).

0143-7208/$ – see front matter © 2014 Elsevier Ltd. All rights reserved.
http://dx.doi.org/10.1016/j.dyepig.2013.12.025

toward this end is to introduce more π-conjugation segments between the donor and acceptor, thereby forming D–π–π–A structures [44,45]. However, such rod-like molecules may facilitate the recombination of electrons to the triodide and the formation of aggregates between molecules [14]. Therefore, a further improvement could be made by introducing auxiliary electron donor triarylamine antennas into the molecule to form the D–D–π–A structure, which avoids the charge recombination processes of injected electrons with triiodide in the electrolyte and leads to increased open circuit voltage (V_{oc}) [46–50] reported by some groups. These studies suggested that superior performance of organic dyes based on D–D–π–A structure over the simple D–π–A configuration can be achieved by molecular design. Carbazole is a potential hole transport semiconductor in organic devices, presenting unique electronic and optical properties. Therefore, carbazole based organic dyes have attracted broad interest in organic light-emitting diodes (OLEDs) and DSSCs [33,34,51–53]. Triarylamine has been widely used in opto- and electro-active materials for its good electron donating and transporting capability, as well as its special propeller starburst molecular structure [54]. Organic photovoltaic functional materials with such triarylamine as electron donor have aroused great interest and become the focus of intensive research in the field of solar cells. These materials have significantly reinforced the conversion efficiency of the next-generation solar cells, especially for dye sensitized solar cells [54]. The combination of carbazole and triarylamine will provide more effective electron density from carbazole to the triarylamine donor centre [55]. When carbazole carrying lateral alkyl chains, it was found that such groups help to form a blocking layer to keep I_3^- ions away from the TiO_2 electrode surface, hence increasing the electron lifetime and open circuit voltage (V_{oc}) [56]. Also, the thiophene and furan moiety are expected to provide effective conjugation and lower the energy of the charge transfer transition due to their small resonance energies (thiophene, 29 kcal/mol; furan, 16 kcal/mol) [57]. It is therefore interesting to incorporate carbazole, triarylamine and a furan or thiophene moiety. In this study, four new organic dyes **K1**–**K4** have been designed and synthesized through the modification of simple carbazole-π-spacer dyes with auxiliary electron donor and linear or branched long alkyl groups (Fig. 1). These four new sensitizers have been applied successfully to sensitization of nanocrystalline TiO_2-based solar cells and their corresponding photovoltaic properties, electronic and optical properties were investigated in detail.

2. Experimental section

2.1. Materials and reagents

3,6-diiodo-9*H*-carbazole and 1-Propyl-3-methylimidazolium iodide (PMII) were prepared according to the published procedures [58,59]. Methoxypropionitrile (MPN), tetra-n-butylammonium hexafluorophosphate ($TBAPF_6$), 4-*tert*-butylpyridine (TBP), lithium iodide and iodine were purchased from Aldrich. Transparent FTO conducting glass (fluorine doped SnO_2, transmission > 90% in the visible, sheet resistance 15 Ω/square) was obtained from the Nippon Sheet Glass Co., Ltd. All other chemicals and solvents used in this work were of reagent grade and used without further purification unless otherwise noted.

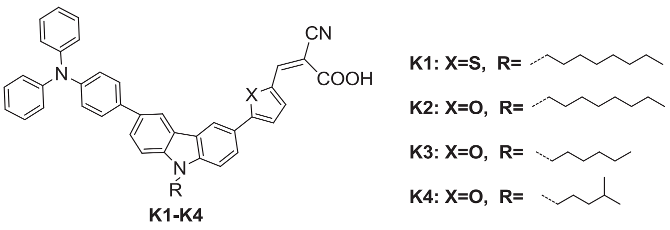

Fig. 1. Molecular structures of carbazole dyes (**K1**–**K4**).

2.2. Characterization

^1H NMR and ^{13}C NMR spectra were recorded on Bruker AM 400 MHz instruments and spectra were referenced against tetramethylsilane as the internal standard. Mass spectra were performed using a ThermoFinnigan LCQ quadrupole ion trap mass spectrometer. The absorption spectra of the organic dyes either in solution or the adsorbed TiO_2 films were measured with a UV-1800 spectrophotometer (Shimadzu Pte. Ltd.). Cyclic Voltammetry measurements were determined with Autolab potentiostat galvanostat PGSTAT30 differential electrometer amplifier using a three-electrode cell with a platinum (Pt) working electrode, a Pt wire counter electrode, and a saturated calomel reference electrode (SCE) in saturated KCl solution, 0.1 M $TBAPF_6$ was used as the supporting electrolyte in dichloromethane (DCM). The ferrocenium/ferrocene (Fc/Fc^+) redox couple was used as an internal potential reference. The $E_{1/2}$ of the Fc/Fc^+ redox couple was found to be 0.50 V versus the SCE reference electrode or 0.74 V versus the normal hydrogen electrode (NHE).

2.3. Synthesis of dyes

2.3.1. 3,6-Diiodo-9-octyl-9H-carbazole (1)

A mixture of 3,6-diiodo-9*H*-carbazole (2.00 g, 4.77 mmol), 1-bromooctane (1.10 g, 5.70 mmol) and potassium 2-methylpropan-2-olate (0.64 g, 5.70 mmol) in dimethylformamide (DMF) (15 ml) were stirred under room temperature for 12 h. The mixture was poured into water and extracted with CH_2Cl_2 (3 × 10 ml). The combined organic layers were dried with anhydrous $MgSO_4$. The solvent was evaporated, and the residue was purified by column chromatography on silica gel (hexane) to give a colorless solid (yield 88%). ^{1}HNMR($CDCl_3$, 400 MHz), δ 8.32 (s, 2H), 7.71 (d, $J = 8.0$ Hz, 2H), 7.17 (D, $J = 8.0$ Hz, 2H), 4.21 (t, $J = 8.0$ Hz, 2H), 1.84–1.77 (m, 2H), 1.30–1.23 (m, 10H), 0.86 (t, J = 8.0 Hz, 3H). ^{13}CNMR($CDCl_3$, 100 MHz), δ 139.49, 134.48, 129.34, 123.96, 110.88, 81.61, 43.23, 31.72, 29.09, 27.19, 22.55, 14.03. MS (ESI, *m*/*z*) calcd for $C_{20}H_{24}I_2N$ $[M + H]^+$: 532.00, Found: 531.90.

2.3.2. 3,6-Diiodo-9-hexyl-9H-carbazole (2)

The synthesis method resembles that of compound **1** but with 1-bromohexane instead (0.78 g, 4.73 mmol) of 1-bromooctane, and the compound was purified by column chromatography on silica gel (hexane) to yield 3.4 g of colorless solid (yield 86%). ^{1}H NMR ($CDCl_3$, 400 MHz), δ 8.34 (s, 2H), 7.74 (d, J = 8.8 Hz, 2H), 7.19 (d, $J = 8.8$ Hz, 2H), 4.23 (t, $J = 7.2$ Hz, 2H), 1.88–1.79 (m, 2H), 1.37–1.29 (m, 6H), 0.88 (t, J = 7.0 Hz, 3H). MS (ESI, *m*/*z*) calcd for $C_{18}H_{20}$ I_2N $[M + H]^+$: 503.97, Found: 503.68.

2.3.3. 3,6-Diiodo-9-(4-methylpentyl)-9H-carbazole (3)

The synthesis method resembles that of compound **1** but with 1-bromo-4-methylpentane (0.78 g, 4.73 mmol) instead of 1-bromooctane, and the compound was purified by column chromatography on silica gel (hexane) to yield 2.7 g of colorless solid (yield 82%). ^{1}H NMR ($CDCl_3$, 400 MHz), δ 8.32 (s, 2H), 7.72 (d, J = 8.4 Hz, 2H), 7.16 (d, $J = 8.4$ Hz, 2H), 4.18 (t, $J = 7.4$ Hz, 2H), 1.86–1.78 (m, 2H), 1.61–1.54 (m, 1H), 1.30–1.22 (m, 2H), 0.88 (d, $J = 6.4$ Hz, 6H). MS (ESI, *m*/*z*) calcd for $C_{18}H_{20}$ I_2N $[M + H]^+$: 503.97, Found: 503.68.

2.3.4. 5-(6-Iodo-9-octyl-9H-carbazol-3-yl)thiophene-2-carbaldehyde (4)

A mixture of **1** (100 mg, 0.19 mmol), $Pd(PPh_3)_4$ (20 mg, 0.017 mmol), and K_2CO_3 (1.02 g, 0.01 mol) in THF (8 ml) and water

(5 ml) were heated to 45 °C under an nitrogen atmosphere for 30 min. 5-formylthiophen-2-ylboronic acid (30 mg, 0.19 mmol) in THF (3 ml) was added, and the mixture was heated under refluxed for a further 18 h. After cooling to room temperature, THF was evaporated and the mixture was extracted with CH_2Cl_2 (3 × 10 ml). The combined organic layers were dried with anhydrous $MgSO_4$. The solvent was evaporated, and the residue was purified by column chromatography on silica gel (hexane/DCM = 2/1, V/V) to give a yellow solid (yield 25%). ^{1}H NMR ($CDCl_3$, 400 MHz), δ 9.89 (s, 1H), 8.44 (s, 1H), 8.33 (s, 1H), 7.79 (d, $J = 8.0$ Hz, 1H), 7.76 (d, $J = 4.0$ Hz, 1H), 7.74 (d, $J = 8.0$ Hz, 1H), 7.44 (d, $J = 4.0$ Hz, 1H), 7.42 (d, $J = 8.0$ Hz, 1H), 7.21 (d, $J = 8.0$ Hz, 1H), 4.28 (t, $J = 8.0$ Hz, 2H), 1.88–1.82 (m, 2H), 1.33–1.23 (m, 10H), 0.86 (t, $J = 8.0$ Hz, 3H). MS (ESI, m/z) calcd for $C_{25}H_{27}INOS$ $[M + H]^+$: 516.09, Found: 516.10.

2.3.5. 5-(6-Iodo-9-octyl-9H-carbazol-3-yl)furan-2-carbaldehyde (*5*)

The synthesis method resembles that of compound **4** but 5-formylfuran-2-ylboronic acid (26 mg, 0.18 mmol) instead of 5-formylthiophen-2-ylboronic acid, and the compound was purified by column chromatography on silica gel (hexane/DCM = 2/1, V/V) to yield 154 mg of yellow solid (yield 30%). ^{1}H NMR ($CDCl_3$, 400 MHz), δ 9.64 (s, 1H), 8.50 (s, 1H), 8.46 (s, 1H), 7.93 (d, $J = 8.0$ Hz, 1H), 7.74 (d, $J = 8.0$ Hz, 1H), 7.42 (d, $J = 8.0$ Hz, 1H), 7.36 (d, $J = 4.0$ Hz, 1H), 7.20 (d, $J = 8.0$ Hz, 1H), 6.84 (d, $J = 4.0$ Hz, 1H), 4.27 (t, $J = 8.0$ Hz, 2H), 1.89–1.82 (m, 2H), 1.33–1.23 (m, 10H), 0.86 (t, $J = 8.0$ Hz, 3H). MS (ESI, m/z) calcd for $C_{25}H_{27}INO_2$ $[M + H]^+$: 500.11, Found: 500.20.

2.3.6. 5-(9-Hexyl-6-iodo-9H-carbazol-3-yl)furan-2-carbaldehyde (*6*)

The synthesis method resembles that of compound **4** but **2** instead of **1**, and the compound was purified by column chromatography on silica gel (hexane/DCM = 2/1, V/V) to yield 170 mg of yellow solid (yield 37%). ^{1}H NMR ($CDCl_3$, 400 MHz), δ 9.65 (s, 1H), 8.48 (d, $J = 8.4$ Hz, 2H), 7.92 (d, $J = 6.8$ Hz, 1H), 7.74 (d, $J = 6.8$ Hz, 1H), 7.42 (d, $J = 6.8$ Hz, 1H), 7.38 (d, $J = 2.8$ Hz, 1H), 7.20 (d, $J = 6.8$ Hz, 1H), 6.86 (d, $J = 3.2$ Hz, 1H), 4.26 (t, $J = 5.8$ Hz, 2H), 1.91–1.83 (m, 2H), 1.38–1.29 (m, 6H), 0.88 (t, $J = 5.6$ Hz, 3H). MS (ESI, m/z) calcd for $C_{23}H_{23}INO_2$ $[M + H]^+$: 472.08, Found: 472.10.

2.3.7. 5-(6-Iodo-9-(4-methylpentyl)-9H-carbazol-3-yl)furan-2-carbaldehyde (*7*)

The synthesis method resembles that of compound **6** but **3** instead of **1**, and the compound was purified by column chromatography on silica gel (hexane/DCM = 2/1, V/V) to yield 160 mg of yellow solid (yield 21%). ^{1}H NMR ($CDCl_3$, 400 MHz), δ 9.65 (s, 1H), 8.46 (d, $J = 8.4$ Hz, 2H), 7.92 (d, $J = 6.8$ Hz, 1H), 7.74 (d, $J = 6.8$ Hz, 1H), 7.40 (d, $J = 6.8$ Hz, 1H), 7.37 (d, $J = 2.8$ Hz, 1H), 7.19 (d, $J = 6.8$ Hz, 1H), 6.84 (d, $J = 2.8$ Hz, 1H), 4.23 (t, $J = 5.8$ Hz, 2H), 1.89–1.83 (m, 2H), 1.64–1.54 (m, 1H), 1.29–1.25 (m, 2H), 0.88 (d, $J = 2.8$ Hz, 6H). MS (ESI, m/z) calcd for $C_{23}H_{23}INO_2$ $[M + H]^+$: 472.08, Found: 472.10.

2.3.8. 5-(6-(4-(Diphenylamino)phenyl)-9-octyl-9H-carbazol-3-yl)thiophene-2-carbaldehyde (*8*)

A mixture of **4** (100 mg, 0.194 mmol), $Pd(PPh_3)_4$ (10 mg, 0.009 mmol), 4-(diphenylamino)phenylboronic acid (56 mg, 0. 0.194 mmol) and toluene (5 ml) were stirred under an nitrogen atmosphere. K_2CO_3 (1.02 g, 0.01 mol) in H_2O (5 ml) was injected to the solution and the mixture was heated under reflux for a further 12 h. After cooling to room temperature, the mixture was extracted with CH_2Cl_2 (3 × 10 ml). The combined organic layers were dried with anhydrous $MgSO_4$. The solvent was evaporated, and the residue was purified by column chromatography on silica gel (hexane/DCM = 2/1, v/v) to give a yellow solid in 86% yield. ^{1}H NMR ($CDCl_3$, 400 MHz), δ 9.89 (s, 1H), 8.44 (s, 1H), 8.32 (s, 1H), 7.90 (d, $J = 8.0$ Hz, 1H), 7.76 (d, $J = 4.0$ Hz, 1H), 7.74 (d, $J = 8.0$ Hz, 1H), 7.61 (d, $J = 8.0$ Hz, 2H), 7.48–7.43 (m, 3H), 7.29 (t, $J = 8.0$ Hz, 4H), 7.21–7.16 (m, 6H), 7.04 (t, $J = 8.0$ Hz, 2H), 4.33 (t, $J = 8.0$ Hz, 2H), 1.94–1.87 (m, 2H), 1.39–1.25 (m, 10H), 0.86 (t, $J = 8.0$ Hz, 3H). MS (ESI, m/z) calcd for $C_{43}H_{41}N_2OS$ $[M + H]^+$: 633.29, Found: 633.15.

2.3.9. 5-(6-(4-(Diphenylamino)phenyl)-9-octyl-9H-carbazol-3-yl)furan-2-carbaldehyde (*9*)

The synthesis method resembles that of compound **8** but **5** instead of **4**, and the compound was purified by column chromatography on silica gel (hexane/DCM = 2/1, V/V) to give 160 mg of orange solid in 81% yield. ^{1}H NMR ($CDCl_3$, 400 MHz), δ 9.66 (s, 1H), 8.66 (s, 1H), 8.39 (s, 1H), 7.94 (d, $J = 6.8$ Hz, 1H), 7.76 (d, $J = 6.8$ Hz, 1H), 7.64 (d, $J = 6.8$ Hz, 2H), 7.48–7.44 (m, 2H), 7.40 (s, 1H), 7.32 (t, $J = 6.2$ Hz, 4H), 7.24–7.19 (m, 6H), 7.07 (t, $J = 5.8$ Hz, 2H), 6.88 (s, 1H), 4.35 (t, $J = 8.0$ Hz, 2H), 1.97–1.88 (m, 2H), 1.46–1.28 (m, 10H), 0.89 (t, $J = 6.0$ Hz, 3H). MS (ESI, m/z) calcd for $C_{43}H_{41}N_2O_2$ $[M + H]^+$: 617.32, Found: 617.35.

2.3.10. 5-(6-(4-(Diphenylamino)phenyl)-9-hexyl-9H-carbazol-3-yl)furan-2-carbaldehyde (*10*)

The synthesis method resembles that of compound **8** but **6** instead of **4**, and the compound was purified by column chromatography on silica gel (hexane/DCM = 2/1, V/V) to give 120 mg of orange solid in 88% yield. ^{1}H NMR ($CDCl_3$, 400 MHz), δ 9.66 (s, 1H), 8.65 (s, 1H), 8.39 (s, 1H), 7.93 (d, $J = 7.2$ Hz, 1H), 7.76 (d, $J = 7.2$ Hz, 1H), 7.64 (d, $J = 6.8$ Hz, 2H), 7.48 (d, $J = 6.8$ Hz, 2H), 7.46 (d, $J = 6.8$ Hz, 2H), 7.38 (d, $J = 2.8$ Hz, 1H), 7.32 (t, $J = 6.2$ Hz, 4H), 7.25–7.20 (m, 6H), 7.07 (t, $J = 6.0$ Hz, 2H), 6.88 (d, $J = 2.8$ Hz, 1H), 4.34 (t, $J = 5.6$ Hz, 2H), 1.96–1.90 (m, 2H), 1.46–1.30 (m, 6H), 0.91 (t, $J = 5.6$ Hz, 3H). MS (ESI, m/z) calcd for $C_{41}H_{37}N_2O_2$ $[M + H]^+$: 589.29, Found: 589.35.

2.3.11. 5-(6-(4-(Diphenylamino)phenyl)-9-(4-methylpentyl)-9H-carbazol-3-yl)furan-2-carbaldehyde (*11*)

The synthesis method resembles that of compound **8** but **7** instead of **4**, and the compound was purified by column chromatography on silica gel (hexane/DCM = 2/1, V/V) to yield 180 mg of orange solid (yield 79%). ^{1}H NMR ($CDCl_3$, 400 MHz), δ 9.66 (s, 1H), 8.64 (s, 1H), 8.40 (s, 1H), 7.94 (d, $J = 6.8$ Hz, 1H), 7.76 (d, $J = 6.8$ Hz, 1H), 7.65 (d, $J = 6.8$ Hz, 2H), 7.47 (d, $J = 6.8$ Hz, 1H), 7.45 (d, $J = 7.2$ Hz, 1H), 7.38 (d, $J = 2.8$ Hz, 1H), 7.32 (t, $J = 6.2$ Hz, 4H), 7.25–7.20 (m, 6H), 7.08(t, $J = 5.8$ Hz, 2H), 6.87 (d, $J = 2.8$ Hz, 1H), 4.31 (t, $J = 5.8$ Hz, 2H), 1.96–1.90 (m, 2H), 1.66–1.60 (m, 1H), 1.36–1.30 (m, 2H), 0.92 (d, $J = 5.2$ Hz, 6H). MS (ESI, m/z) calcd for $C_{41}H_{37}N_2O_2$ $[M + H]^+$: 589.29, Found: 589.35.

2.3.12. 2-Cyano-3-(5-(6-(4-(diphenylamino)phenyl)-9-octyl-9H-carbazol-3-yl)thiophen-2-yl)acrylic acid (*K1*)

A mixture of **8** (60 mg, 0.095 mmol), 2-cyanoacetic acid (40 mg, 0.45 mmol), ammonium acetate (50 mg) and acetic acid (8 ml) were heated at 120 °C under an argon atmosphere for 12 h. After cooling to room temperature, the mixture was added to water. The precipitate was filtered and washed with water. The residue was purified by column chromatography on silica gel (DCM/EtOH = 20/1, v/v) to give a red solid (yield 87%). ^{1}H NMR(400 MHz, THF-d_8), δ 8.49 (s, 1H), 8.43 (s, 1H), 8.34 (d, $J = 8.4$ Hz, 1H), 7.74 (t, $J = 7.8$ Hz, 3H), 7.66 (d, $J = 7.2$ Hz, 2H), 7.49 (s, 2H), 7.26 (t, $J = 7.2$ Hz, 4H), 7.18–7.12 (m, 7H), 7.01 (t, $J = 7.0$ Hz, 2H), 4.28 (t, $J = 7.2$ Hz, 2H), 1.90–1.80 (m, 2H), 1.33–1.22 (m, 10H), 0.87 (t, $J = 6.8$ Hz, 3H). ^{13}C NMR (THF-d_8, 100 MHz), δ 161.3, 148.2, 147.9, 146.4, 141.1, 140.1, 136.4, 134.8, 129.0, 127.6, 124.5, 124.4, 124.0, 123.3, 122.5, 118.5, 117.9, 109.1, 42.7, 31.8, 29.4, 29.2, 28.9, 27.1, 22.5, 13.4. HRMS (ESI, m/z) calcd for $C_{46}H_{41}N_3O_2S$ $[M-H]^-$: 699.2919, Found: 699.2895.

2.3.13. 2-Cyano-3-(5-(6-(4-(diphenylamino)phenyl)-9-octyl-9H-carbazol-3-yl)furan-2-yl)acrylic acid (**K2**)

A procedure similar to that for the dye **K1** but with compound **9** (120 mg, 0.17 mmol) instead of compound **8** giving the dye **K2** as a dark red solid (yield 67%). ^{1}H NMR (400 MHz, THF-d_8), δ 8.82 (s, 1H), 8.45 (s, 1H), 8.12 (d, J = 8.4 Hz, 1H), 8.04 (s, 1H), 7.78 (d, J = 8.4 Hz, 1H), 7.70–7.59 (m, 4H), 7.47 (s, 1H), 7.29 (t, J = 8.0 Hz, 4H), 7.21–7.14 (m, 7H), 7.03 (t, J = 7.2 Hz, 2H), 4.44 (t, J = 7.2 Hz, 2H), 1.96–1.93 (m, 2H), 1.46–1.30 (m, 10H), 0.90 (d, J = 7.0 Hz, 3H). ^{13}C NMR (THF-d_8, 100 MHz), δ 161.1, 148.0, 147.7, 146.6, 141.6, 140.4, 136.4, 132.5, 129.0, 127.6, 125.1, 124.4, 124.0, 123.3, 122.5, 120.2, 118.2, 117.8, 109.5, 109.4, 42.9, 31.8, 29.4, 29.2, 29.0, 27.1, 22.5, 13.4. HRMS (ESI, m/z) calcd for $C_{46}H_{41}N_3O_3$ $[M-H]^-$: 683.3148, Found: 683.3092.

2.3.14. 2-Cyano-3-(5-(6-(4-(diphenylamino)phenyl)-9-hexyl-9H-carbazol-3-yl)furan-2-yl)acrylic acid (**K3**)

A procedure similar to that for the dye **K1** but with compound **10** (120 mg, 0.17 mmol) instead of compound **8** giving the dye **K3** as a red solid (yield 58%). ^{1}H NMR (400 MHz, THF-d_8), δ 8.67 (s, 1H), 8.30 (s, 1H), 7.97(d, J = 7.6 Hz, 1H), 7.91 (s, 1H), 7.64 (d, J = 8.4 Hz, 1H), 7.55 (d, J = 8.4 Hz, 2H), 7.45 (d, J = 8.4 Hz, 2H), 7.32 (s, 1H), 7.15 (t, J = 7.8 Hz, 4H), 7.07–7.01 (m, 7H), 6.90 (t, J = 7.2 Hz, 2H), 4.28 (t, J = 7.2 Hz, 2H), 1.82–1.78 (m, 2H), 1.32–1.20 (m, 6H), 0.76 (d, J = 6.6 Hz, 3H). ^{13}C NMR (THF-d_8, 100 MHz), δ 159.4, 146.1, 145.7, 144.7, 139.8, 138.5, 135.2, 134.5, 130.6, 127.2, 125.7, 123.2, 122.5, 122.1, 121.5, 121.4, 120.7, 118.4, 116.4, 115.9, 107.6, 107.5, 105.3, 41.0, 29.7, 27.1, 24.9, 20.6, 11.5. HRMS (ESI, m/z) calcd for $C_{44}H_{37}N_3O_3$ $[M-H]^-$: 655.2835, Found: 655.2806.

2.3.15. 2-Cyano-3-(5-(6-(4-(diphenylamino)phenyl)-9-(4-methylpentyl)-9H-carbazol-3-yl)furan-2-yl)acrylic acid (**K4**)

A procedure similar to that for the dye **K1** but with compound **11** (120 mg, 0.17 mmol) instead of compound **8** giving the dye **K4** as a red solid (yield 56%). ^{1}H NMR(400 MHz, THF-d_8), δ 8.81 (s, 1H), 8.44 (s, 1H), 8.11 (d, J = 7.6 Hz, 1H), 8.05 (s, 1H), 7.78 (d, J = 8.4 Hz, 1H), 7.68 (d, J = 8.4 Hz, 2H), 7.59 (d, J = 8.4 Hz, 2H), 7.45 (s, 1H), 7.29 (t, J = 7.8 Hz, 4H), 7.21–7.14 (m, 7H), 7.03 (t, J = 7.4 Hz, 2H), 4.42 (t, J = 7.2 Hz, 2H), 1.96–1.93 (m, 2H), 1.66–1.59 (m, 1H), 1.38–1.33 (m, 2H), 0.91 (d, J = 6.4 Hz, 6H). ^{13}C NMR (THF-d_8, 100 MHz), δ 159.0, 148.0, 147.6, 146.5, 141.7, 140.3, 136.4, 132.4, 129.0, 127.6, 125.1, 124.4, 124.0, 123.5, 123.4, 123.2, 120.2, 118.2, 117.8, 109.4, 109.3, 43.1, 36.1, 27.9, 26.8, 21.9. HRMS (ESI, m/z) calcd for $C_{44}H_{37}N_3O_3$ $[M-H]^-$: 655.2835, Found: 655.2786.

2.4. Fabrication of DSSCs

The TiO_2 films were fabricated with a screen printing method according to the published method [60]. The thickness is about 15 μm. The TiO_2 electrodes were heated under an air flow at 450 °C for 15 min and 500 °C for 15 min. The sintered films were further treated with 40 mM $TiCl_4$ aqueous solution at room temperature for 12 h and washed with water and ethanol, a process which can significantly increase the short-circuit photocurrent. Because $TiCl_4$ (aqueous) had the effect to remove the iron contamination source, which can quench the dye-sensitized photocurrent (J_{sc}) [61]. Then the films were annealed at 450 °C for 30 min. After the $TiCl_4$ pre-treated films were cooled down at around 50 °C, the films were immersed into a 5×10^{-4} M dye bath in CH_2Cl_2 solutions and maintained under dark for 48 h at room temperature. The electrode was then rinsed with CH_2Cl_2 and ethanol and dried. The size of the TiO_2 electrodes used was 0.28 cm^2. To prepare the counter electrode, the Pt catalyst was deposited on the cleaned FTO glass by spinning with a drop of H_2PtCl_6 solution (20 mM 2-propanol solution) with the heat treatment at 400 °C for 15 min. Two holes (0.8 mm diameter) were drilled on the counter electrode using a drill-press. The perforated sheet was cleaned with ultrasound in an ethanol bath for 10 min. For the assembly of DSSCs, the dye-covered TiO_2 electrode and Pt-counter electrode were assembled into a sandwich type cell and sealed with a hot-melt gasket of 25 μm thickness made of the ionomer Surlyn 1702 (DuPont). The electrolyte was introduced into the cell via backfilling from a hole in the back of the counter electrode. Finally, the hole was sealed using a self-adhesive aluminium film. In this work, two liquid electrolytes were employed: electrolyte A, 0.1 M LiI, 0.03 M I_2, 0.6 M PMII, 0.1 M Guanidine thiocyanate (GuSCN), and 0.5 M TBP in a mixture of acetonitrile and valeronitrile (volume ratio = 7:3); electrolyte B, 0.1 M LiI, 0.05 M I_2, 0.6 M PMII, and 0.5 M TBP in a mixture of acetonitrile and MPN (volume ratio = 7:3).

2.5. Photovoltaic performance measurements

Photocurrent–voltage (J–V) measurements were performed using an AM 1.5 solar simulator (Newport, USA). The solar simulator was calibrated by using a standard silicon cell (Newport, USA). Current–voltage curves were measured using a computer-controlled IV tracer (VS-6810, Industrial Vision Technology (S) Pte Ltd., Singapore). A black mask with an aperture area of 0.1589 cm^2 was used to test cell active area. The photocurrent action spectra were measured with a monochromatic Incident Photon-to-electron Conversion Efficiency (IPCE) test system consisting of a Model SR830 DSP Lock-In Amplifier, a Model SR540 Optical Chopper (Stanford Research Corporation, USA), a 7IL/PX150 xenon lamp with power supply, and a 7ISW301 Spectrometer.

3. Results and discussion

3.1. Synthesis and structural characterization

The synthetic route employed to access four dyes (**K1**–**K4**) is shown in Scheme 1. The dyes were prepared from 3,6-diiodo-9H-carbazole, which was synthesized according to a published procedure [58]. Notably, the alkyl chain on the carbazole group can improve the solubility and form a tightly packed insulating monolayer blocking the I_3^- anions or cations from approaching the TiO_2 surface, thereby retarding the charge recombination processes of injected electrons with I_3^- ions in the electrolyte, which is the main decreasing factor for V_{oc} [33]. Accordingly, we incorporated the carbazole unit with different alkyl groups on the 9-position as an electron donor, cyanoacrylic acid as an electron acceptor, furan or thiophene as a linker and triphenylamine as an auxiliary electron donor into the donor–donor–π–acceptor (D–D–π–A) system. As illustrated in Scheme 1, the target dyes **K1**–**K4** were conveniently prepared by a conventional Suzuki cross-coupling and Knoevenagel condensation reactions. Suzuki coupling between the intermediate **1**–**3** and the corresponding boronic acid of the π-conjunction bridge was carried out using $Pd(PPh_3)_4$ as a catalyst in a mixture of 2 M aqueous K_2CO_3 and THF under reflux conditions to give the corresponding intermediate **4**–**7**. These intermediates were reacted with (4-(diphenylamino)phenyl)boronic acid through a Suzuki coupling reaction using toluene as solvent to provide the corresponding intermediate **8**–**11**. Finally, the target dyes (**K1**–**K4**) were synthesized via Knoevenagel condensation reaction of aldehydes **8**–**11** with cyanoacetic acid in the presence of acetic acid and ammonium acetate. All the intermediates and target dyes were confirmed by standard spectroscopic methods.

3.2. Absorption properties in solutions and on TiO_2 film

The UV–vis absorption spectra of the dyes **K1**–**K4** in DCM and adsorbed on 7 μm transparent TiO_2 films are displayed in Fig. 2. The

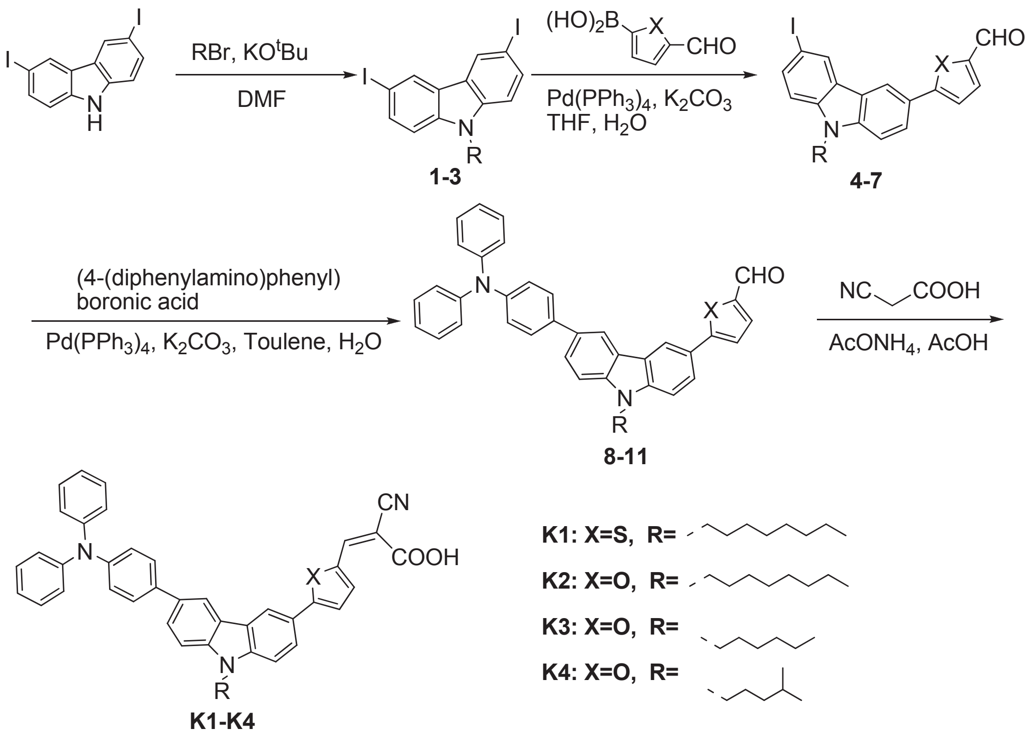

Scheme 1. Synthetic routes of carbazole dyes (**K1**–**K4**).

related photophysical data are summarized in Table 1. The four dyes **K1**–**K4** in DCM exhibit two strong absorption peaks, one at 300–380 nm and the other at around 380–550 nm. The first adsorption band might be ascribed to a localized aromatic π–π^* electron transition of typical triarylamine [48,62]. The second absorption band may be assigned to the intramolecular charge transition (ICT) between the central carbazole (electron donor) and the cyanoacetic acid (electron acceptor and anchoring moiety) [9]. Compared to that of **K1**, the adsorption spectra of **K2**–**K4** are red-shifted by 26 nm together with an increase in molar extinction coefficient, indicating that the furan unit can exhibit a better absorption performance compared to the thiophene unit. This may be caused by the different aromatic ability of the two five-membered heteroaromatic bridges. The aromatic ability of furan is larger than that of thiophene due to the stronger electronegative of oxygen element than of sulfur [63]. As summarized in Table 1, the molar extinction coefficient of **K2**–**K4** are determined to be 36,700, 36,400 and 33,500 M^{-1} cm^{-1}, respectively, which are about 1.22, 1.21 and 1.12 times the corresponding value of **K1**. This may also demonstrate the superiority of a furan conjunction bridge in light harvesting in the visible region. The dye **K2** gives a maximum absorption similar to the dye **K3** and **K4** but its molar extinction coefficient ($\varepsilon = 3.67 \times 104$ M^{-1} cm^{-1}) is higher than those of the dye **K3** ($\varepsilon = 3.647 \times 104$ M^{-1} cm^{-1}) and **K4** ($\varepsilon = 3.35 \times 104$ M^{-1} cm^{-1}), which indicates that the absorption capacity of **K2** can be enhanced by increasing length of alkyl chain. Similar studies with results from increasing alkyl chain have been reported [9,64]. The absorption spectra of **K1**–**K4** adsorbed on the surface of 7 mm transparent TiO_2 films are shown in Fig. 2(b). All dyes show broadened absorption bands as compared to those in solutions, which is beneficial to light-harvesting and thus increase the photocurrent response, leading to an increasing J_{sc} [9]. The maximum absorption peaks for **K1**–**K4** on the TiO_2 film are at 463, 457, 488 and 445 nm, respectively. The red shifts of the λ_{max} of **K1** and **K3** are possible due to the J-aggregation of the dyes on the TiO_2 surface. Such J-aggregation formation may indicate a head-to-tail configuration between the adjacent molecules on the TiO_2 surfaces [64]. The blue-shift in the absorption spectra on the TiO_2 film of **K2** and **K4** might arise by the interaction of the anchoring groups with the TiO_2 surface because of the introduction of alkyl substituted carbazole, which is beneficial to the inhibition of dye aggregation. This TiO_2 surface interaction directly reduces the energy of the π^* level and the formation of J-aggregates on the TiO_2 surface [65].

3.3. Electrochemical properties

To investigate the ability of electron transfer from the excited dye to the conduction band of TiO_2, cyclic voltammetric analysis of the four dyes was performed. Fig. 3 depicts the typical cyclic voltammogram of **K1**–**K4**, the highest occupied molecular orbitals (HOMOs) of **K1**–**K4** corresponding to their first redox potential are 0.95–0.97 V vs. NHE. As estimated from the absorption threshold of these dyes adsorbed onto TiO_2 films, the resulting E_{0-0} is 2.34, 2.31, 2.31 and 2.31 eV for **K1**, **K2**, **K3** and **K4**, respectively. The estimated excited state potential corresponding to the lowest unoccupied molecular orbital (LUMO) levels, calculated from $E_{HOMO} - E_{0-0}$, are −1.38, −1.36, −1.34 and −1.36 V, respectively. The examined HOMO and LUMO levels are listed in Table 1. From these data, it is observed that the HOMO levels of **K1**–**K4** are sufficiently more positive than the iodine/iodide redox potential value (0.4 V vs. NHE), indicating that the oxidized dyes formed after electron injection into the conduction band of TiO_2 could thermodynamically accept electrons from I^- ions. The LUMO levels of these dyes are sufficiently more negative than the conduction-band-edge energy level (E_{cb}) of the TiO_2 electrode (−0.5 V vs. NHE), which implies that electron injection from the excited dye into the conduction band of TiO_2 is energetically permitted [66].

3.4. Photovoltaic device performance

Fig. 4 shows the action spectra of incident photon-to-current conversion efficiency (IPCE) for DSSCs based on the four dyes

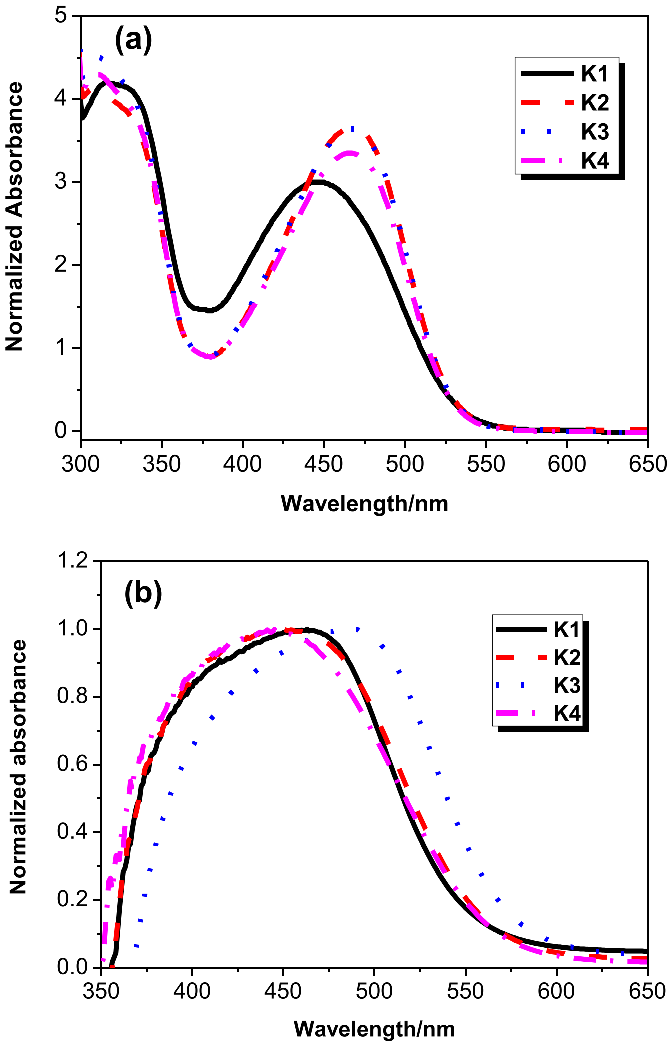

Fig. 2. Normalized UV–Vis absorption spectra of carbazole dyes (**K1**–**K4**) in CH_2Cl_2 solution (a) and on TiO_2 film (b).

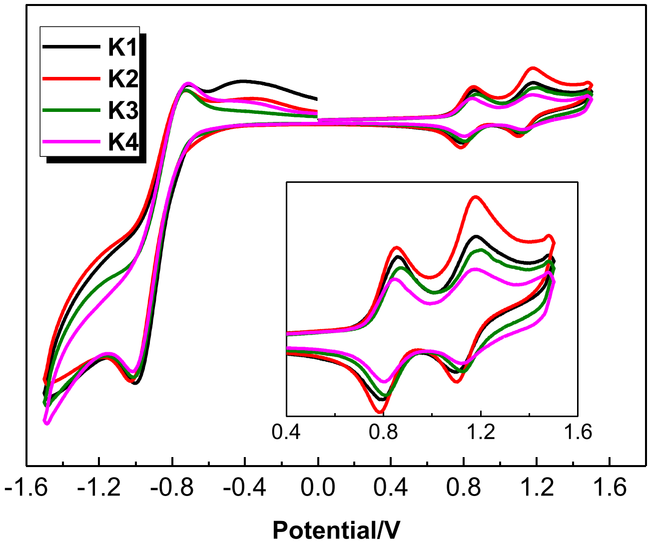

Fig. 3. Cyclic voltammetry plots of **K1**–**K4** attached to a nanocrystalline TiO_2 film deposited on conducting FTO glass.

(**K1**–**K4**). The dye-coated TiO_2 film was used as the working electrode, platinized FTO glass as the counter electrode and 0.6 M PMII, 0.05 M I_2, 0.10 M LiI and 0.5 M TBP in acetonitrile and MPN (volume ratio, 7: 3) mixture solution as the redox electrolyte. The solar cells based on **K1**–**K4** exhibit high IPCE values above 60% in the range of 340 nm to around 540 nm and with the highest value of 76.7% in the range of 480 nm for **K1**, 92.4% in the range of 480 nm for **K2**, 82.4% at 430 nm for **K3** and 79.6% at 420 nm for **K4**, respectively. Maximum IPCE values of the dyes are in the order of **K2** > **K3** > **K4** > **K1**. In general, higher IPCE means higher electron transfer yield [67]. Therefore, introduction of a furan moiety and a longer side chain into dyes has a positive effect on IPCE. Thus, we can infer that the DSSC based on **K2** would generate the highest conversion yield among four dyes; a feather which is supported by the device results. The highest IPCE value of **K2** may be attributed to its higher adsorption and enhanced molar extinction coefficient. This is in good agreement with the absorbance spectra of **K2** in solution.

The current–voltage characteristics of DSSCs fabricated with these dyes (**K1**–**K4**) as sensitizers were measured under standard global AM 1.5 solar light condition. The detailed parameters of short-circuit current density (J_{sc}), open-circuit voltage (V_{oc}), fill factor (FF), and photovoltaic conversion efficiency (η) are summarized in Table 2. Two kinds of electrolyte were employed in the DSSCs application. When electrolyte B is used, the DSSC based on **K2** produces the highest η of 6.68% (J_{sc} = 13.26 mA cm^{-2}, $V_{oc} = 0.724$ V, FF = 0.66), which should be attributed to its best IPCE performance. As seen in the results, the J_{sc} increases from 12.14 mA cm^{-2} to 13.26 mA cm^{-2} by increasing chain length from methylpentyl (**K4**) to octyl (**K2**) for **K2**–**K4**. This behavior of dyes may be due to alkyl chains self-assembling on TiO_2 film and a longer distance between the TiO_2 film and electrolyte by lengthening of the alkyl chains, which block the recapture of the photo-

Table 1
Optical and electrochemical properties of carbazole dyes.

Dye	λ_{max}/nm ($\varepsilon \times 10^4$ M^{-1} cm^{-1})	λ_{onset} (nm)	HOMO/V (*vs.* NHE)	E_{0-0} (eV)	LUMO/V (*vs.* NHE)
K1	442 (3.00)	530	0.96	2.34	−1.38
K2	468 (3.67)	537	0.95	2.31	−1.36
K3	468 (3.64)	537	0.97	2.31	−1.34
K4	468 (3.35)	537	0.95	2.31	−1.36

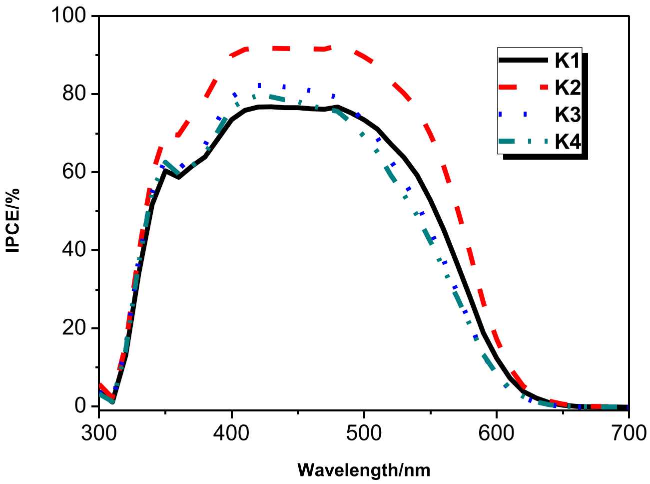

Fig. 4. Photocurrent action spectra of the TiO_2 electrodes sensitized by **K1**–**K4**.

Table 2
Photovoltaic performance of DSSCs based on the carbazole dyes **K1**–**K4** and **N719** with liquid electrolyte A and B.[a]

Dye	Electrolyte	J_{sc} (mA cm^{-2})	V_{oc} (mV)	FF	η (%)
K1	A	9.54	815	0.673	5.23
K1	B	11.12	741	0.678	5.59
K2	A	11.00	786	0.661	6.02
K2	B	13.26	724	0.661	6.68
K3	A	10.85	797	0.644	5.86
K3	B	12.31	737	0.666	6.35
K4	A	10.18	799	0.634	5.43
K4	B	12.14	722	0.655	6.04
N719	A	15.58	783	0.635	7.74
N719	B	14.29	703	0.673	6.98

[a] Illumination: 100 mW cm^{-2} simulated AM 1.5 G solar light; electrolyte containing: A: 0.1 M LiI, 0.6 M PMII, 0.03 M I_2, 0.1 M GuSCN, 0.5 M TBP, in acetonitrile and valeronitrile (7:3); B: 0.1 M LiI, 0.05 M I_2, 0.6 M PMII, 0.5 M TBP in the mixed solvent of acetonitrile and MPN (7:3, v/v).

injected electrons by triodide ions [9]. Compared to **K2**, **K3** and **K4**, **K1** has a lower J_{sc} value, indicating that furan moiety may have better charge carrier mobility than the thiophene moiety [68]. This result may be due to the low resonance energy of the furan moiety [57,69]_ENREF_71. This trend of J_{sc} (**K2** > **K3** > **K4** > **K1**) is in good accordance with the order of IPCE values and absorbance maxima of the dyes in solution. A similar trend was also observed in J_{sc} when electrolyte A was used. But the values of J_{sc} of **K1**–**K4** using electrolyte B are better than those based on electrolyte A. This result is different in complex ruthenium dye **N719** (Fig. 5), indicating that electrolyte B benefits the IPCE value for organic dyes. However, the V_{oc} values of the DSSCs based on electrolyte B are decreased compared to that of electrolyte A. It was proposed that the dissociated positive Ti^{4+} ions and protons in electrolyte B can be adsorbed onto the surface of TiO_2 and hence the conduction band of TiO_2 is possible to undergo a positive shift. Similar phenomena have already been reported in the case of adding additives in the electrolyte, such as lithium ions, alkali ions and TBP, which are generally believed to affect the surface properties and the electrochemical potentials of TiO_2 [67]. It is also noteworthy that all of carbazole dyes have higher open circuit voltages than N719 measured with two electrolytes under the same measurement conditions, which indicates that the introduction of the alkyl chains into the carbazole moiety can inhibit the charge recombination and improve V_{oc}.

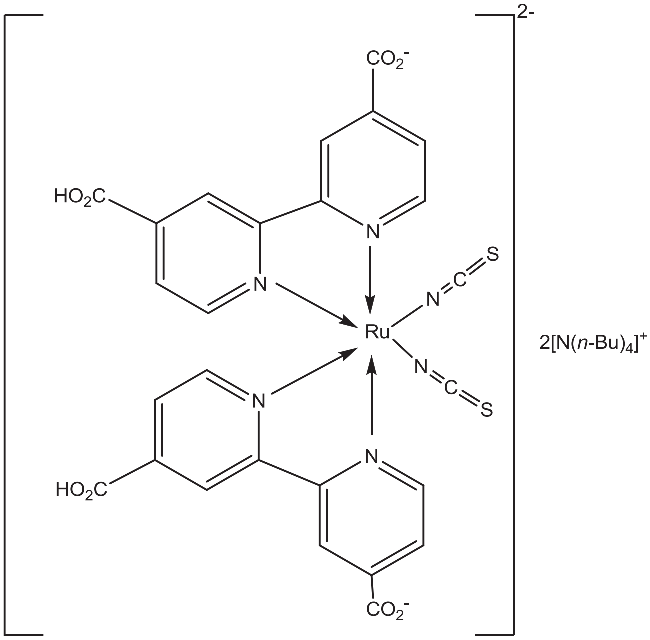

Fig. 5. Molecular structure of **N719**.

Conclusions

In summary, we have designed and synthesized four new carbazole-based metal-free dyes, in which linear or branched alkyl side chains were introduced into to the conjugated system to form a blocking layer. The electron-donating groups of triphenylamine increase the electron density of the donor moiety and enhance the molar extinction coefficient of the dyes. The furan or thiophene linker was introduced to enhance the molar extinction coefficient of dyes. The results based on photovoltaic experiments show that the four dyes exhibit a high open circuit voltage (0.72–0.83 V). The photovoltaic performance of **K2** in DSSCs demonstrates the best overall conversion efficiency of 6.68%, 86.3% of the standard cell from **N719** (7.74%) under the same testing conditions. The results indicate that the introduction of a longer alkyl chain into the carbazole moiety will retard recombination and the introduction of furan as the conjugate bridge will increase the photocurrent response; features which lead to enhanced J_{sc}. Therefore, we conclude that the introduction of both octyl-substituted carbazole and a furan moiety into DSSC can improve the cell efficiency significantly. It was expected that, by adjusting the molecular structure of this kind of carbazole-based metal-free dyes, higher efficiency could be achieved.

Acknowledgment

We would like to thank Ministry of Education, Singapore (tier 1 research grant MOE2008-IF-1-016), Singapore Polytechnic (Idea Fund R733 and R734) for the financial support and Everlight Chemical Industrial Co. for gifts of materials.

References

[1] O'Regan B, Gratzel M. A low-cost, high-efficiency solar cell based on dye-sensitized colloidal TiO_2 films. Nature 1991;353:737–40.
[2] Gao F, Wang Y, Zhang J, Shi D, Wang M, Humphry-Baker R, et al. A new heteroleptic ruthenium sensitizer enhances the absorptivity of mesoporous titania film for a high efficiency dye-sensitized solar cell. Chem Commun 2008;44:2635–7.
[3] Yum J-H, Jung I, Baik C, Ko J, Nazeeruddin MK, Gratzel M. High efficient donor-acceptor ruthenium complex for dye-sensitized solar cell applications. Energ Environ Sci 2009;2:100–2.
[4] Wang P, Zakeeruddin SM, Moser JE, Nazeeruddin MK, Sekiguchi T, Gratzel M. A stable quasi-solid-state dye-sensitized solar cell with an amphiphilic ruthenium sensitizer and polymer gel electrolyte. Nat Mater 2003;2:402–7.
[5] Zhang G, Bala H, Cheng Y, Shi D, Lv X, Yu Q, et al. High efficiency and stable dye-sensitized solar cells with an organic chromophore featuring a binary [small pi]-conjugated spacer. Chem Commun 2009;45:2198–200.
[6] Qu S, Wu W, Hua J, Kong C, Long Y, Tian H. New diketopyrrolopyrrole (DPP) dyes for efficient dye-sensitized solar cells. J Phys Chem C 2009;114:1343–9.
[7] Kim D, Lee JK, Kang SO, Ko J. Molecular engineering of organic dyes containing N-aryl carbazole moiety for solar cell. Tetrahedron 2007;63:1913–22.
[8] Tian H, Yang X, Chen R, Pan Y, Li L, Hagfeldt A, et al. Phenothiazine derivatives for efficient organic dye-sensitized solar cells. Chem Commun 2007;43:3741–3.
[9] Iqbal Z, Wu W-Q, Kuang D-B, Wang L, Meier H, Cao D. Phenothiazine-based dyes with bilateral extension of π-conjugation for efficient dye-sensitized solar cells. Dyes Pigm 2013;96:722–31.
[10] Wu W, Yang J, Hua J, Tang J, Zhang L, Long Y, et al. Efficient and stable dye-sensitized solar cells based on phenothiazine sensitizers with thiophene units. J Mater Chem 2010;20:1772–9.
[11] Ma X, Hua J, Wu W, Jin Y, Meng F, Zhan W, et al. A high-efficiency cyanine dye for dye-sensitized solar cells. Tetrahedron 2008;64:345–50.
[12] Funabiki K, Mase H, Hibino A, Tanaka N, Mizuhata N, Sakuragi Y, et al. Synthesis of a novel heptamethine-cyanine dye for use in near-infrared active dye-sensitized solar cells with porous zinc oxide prepared at low temperature. Energ Environ Sci 2011;4:2186–92.
[13] Sayama K, Hara K, Ohga Y, Shinpou A, Suga S, Arakawa H. Significant effects of the distance between the cyanine dye skeleton and the semiconductor surface on the photoelectrochemical properties of dye-sensitized porous semiconductor electrodes. New J Chem 2001;25:200–2.

[14] Tang J, Wu W, Hua J, Li J, Li X, Tian H. Starburst triphenylamine-based cyanine dye for efficient quasi-solid-state dye-sensitized solar cells. Energ Environ Sci 2009;2:982–90.

[15] Sayama K, Hara K, Mori N, Satsuki M, Suga S, Tsukagoshi S, et al. Photosensitization of a porous TiO electrode with merocyanine dyes containing a carboxyl group and a long alkyl chain. Chem Commun 2000;36:1173–4.

[16] Sayama K, Tsukagoshi S, Mori T, Hara K, Ohga Y, Shinpou A, et al. Efficient sensitization of nanocrystalline TiO_2 films with cyanine and merocyanine organic dyes. Sol Energ Mat Sol C 2003;80:47–71.

[17] Hara K, Sato T, Katoh R, Furube A, Ohga Y, Shinpo A, et al. Molecular design of coumarin dyes for efficient dye-sensitized solar cells. J Phys Chem B 2002;107:597–606.

[18] Hara K, Wang Z-S, Sato T, Furube A, Katoh R, Sugihara H, et al. Oligothiophene-containing coumarin dyes for efficient dye-sensitized solar cells. J Phys Chem B 2005;109:15476–82.

[19] Wang ZS, Cui Y, Hara K, Dan-oh Y, Kasada C, Shinpo A. A high-light-harvesting-efficiency coumarin dye for stable dye-sensitized solar cells. Adv Mater 2007;19:1138–41.

[20] Cheng X, Sun S, Liang M, Shi Y, Sun Z, Xue S. Organic dyes incorporating the cyclopentadithiophene moiety for efficient dye-sensitized solar cells. Dyes Pigm 2012;92:1292–9.

[21] Howie WH, Claeyssens F, Miura H, Peter LM. Characterization of solid-state dye-sensitized solar cells utilizing high absorption coefficient metal-free organic dyes. J Am Chem Soc 2008;130:1367–75.

[22] Kuang D, Uchida S, Humphry-Baker R, Zakeeruddin SM, Grätzel M. Organic dye-sensitized ionic liquid based solar cells: remarkable enhancement in performance through molecular design of indoline sensitizers. Angew Chem Int Ed 2008;47:1923–7.

[23] Dentani T, Kubota Y, Funabiki K, Jin J, Yoshida T, Minoura H, et al. Novel thiophene-conjugated indoline dyes for zinc oxide solar cells. New J Chem 2009;33:93–101.

[24] Zhu W, Wu Y, Wang S, Li W, Li X, Chen J, et al. Organic D-A-π-A solar cell sensitizers with improved stability and spectral response. Adv Funct Mater 2011;21:756–63.

[25] Liu B, Zhu W, Zhang Q, Wu W, Xu M, Ning Z, et al. Conveniently synthesized isophorone dyes for high efficiency dye-sensitized solar cells: tuning photovoltaic performance by structural modification of donor group in donor-[small pi]-acceptor system. Chem Commun 2009;45:1766–8.

[26] Liu B, Wu W, Li X, Li L, Guo S, Wei X, et al. Molecular engineering and theoretical investigation of organic sensitizers based on indoline dyes for quasi-solid state dye-sensitized solar cells. Phys Chem Chem Phys 2011;13:8985–92.

[27] Wang Z-S, Li F-Y, Huang C-H. Highly efficient sensitization of nanocrystalline TiO films with styryl benzothiazolium propylsulfonate. Chem Commun 2000;36:2063–4.

[28] Stathatos E, Lianos P, Laschewsky A, Ouari O, Van Cleuvenbergen P. Synthesis of a hemicyanine dye bearing two carboxylic groups and its use as a photosensitizer in dye-sensitized photoelectrochemical cells. Chem Mater 2001;13:3888–92.

[29] Cui Y, Wu Y, Lu X, Zhang X, Zhou G, Miapeh FB, et al. Incorporating benzotriazole moiety to construct D–A–π–A organic sensitizers for solar cells: significant enhancement of open-circuit photovoltage with long alkyl group. Chem Mater 2011;23:4394–401.

[30] Tian H, Yang X, Chen R, Hagfeldt A, Sun L. A metal-free “black dye” for panchromatic dye-sensitized solar cells. Energ Environ Sci 2009;2:674–7.

[31] Gupta KSV, Suresh T, Singh SP, Islam A, Han L, Chandrasekharam M. Carbazole based A-π-D-π-A dyes with double electron acceptor for dye-sensitized solar cell. Organic Electronics.

[32] Tan L-L, Xie L-J, Shen Y, Liu J-M, Xiao L-M, Kuang D-B, et al. Novel organic dyes incorporating a carbazole or dendritic 3,6-diiodocarbazole unit for efficient dye-sensitized solar cells. Dyes Pigm 2014;100:269–77.

[33] Koumura N, Wang Z-S, Mori S, Miyashita M, Suzuki E, Hara K. Alkyl-functionalized organic dyes for efficient molecular photovoltaics. J Am Chem Soc 2006;128:14256–7.

[34] Wang Z-S, Koumura N, Cui Y, Takahashi M, Sekiguchi H, Mori A, et al. Hexylthiophene-functionalized carbazole dyes for efficient molecular photovoltaics: tuning of solar-cell performance by structural modification. Chem Mater 2008;20:3993–4003.

[35] Lai L-F, Qin C, Chui C-H, Islam A, Han L, Ho C-L, et al. New fluorenone-containing organic photosensitizers for dye-sensitized solar cells. Dyes Pigm 2013;98:428–36.

[36] Fakis M, Dori M, Stathatos E, Chou H-H, Yen Y-S, Lin JT, et al. Electron injection in TiO_2 films and quasi-solid state solar cells sensitized with a dipolar fluorene organic dye. J Photochem Photobiology Chem 2013;251:18–24.

[37] Singh P, Baheti A, Thomas KRJ, Lee C-P, Ho K-C. Fluorene-based organic dyes containing acetylene linkage for dye-sensitized solar cells. Dyes Pigm 2012;95:523–33.

[38] Zeng W, Cao Y, Bai Y, Wang Y, Shi Y, Zhang M, et al. Efficient dye-sensitized solar cells with an organic photosensitizer featuring orderly conjugated ethylenedioxythiophene and dithienosilole blocks. Chem Mater 2010;22:1915–25.

[39] Li L, Hao Y, Yang X, Zhao J, Tian H, Teng C, et al. A Double-band tandem organic dye-sensitized solar cell with an efficiency of 11.5 %. ChemSusChem 2011;4:609–12.

[40] Yella A, Lee H-W, Tsao HN, Yi C, Chandiran AK, Nazeeruddin MK, et al. Porphyrin-sensitized solar cells with cobalt (II/III)–based redox electrolyte exceed 12 percent efficiency. Science 2011;334:629–34.

[41] Wu T-Y, Tsao M-H, Chen F-L, Su S-G, Chang C-W, Wang H-P, et al. Synthesis and characterization of organic dyes containing various donors and acceptors. Int J Mol Sci 2010;11:329–53.

[42] Bai Y, Yu Q, Cai N, Wang Y, Zhang M, Wang P. High-efficiency organic dye-sensitized mesoscopic solar cells with a copper redox shuttle. Chem Commun 2011;47:4376–8.

[43] Numata Y, Ashraful I, Shirai Y, Han L. Preparation of donor-acceptor type organic dyes bearing various electron-withdrawing groups for dye-sensitized solar cell application. Chem Commun 2011;47:6159–61.

[44] Chen R, Yang X, Tian H, Sun L. Tetrahydroquinoline dyes with different spacers for organic dye-sensitized solar cells. J Photochem Photobiol A 2007;189:295–300.

[45] Chen R, Yang X, Tian H, Wang X, Hagfeldt A, Sun L. Effect of tetrahydroquinoline dyes structure on the performance of organic dye-sensitized solar cells. Chem Mater 2007;19:4007–15.

[46] Baheti A, Singh P, Lee C-P, Thomas KRJ, Ho K-C. 2,7-diaminofluorene-based organic dyes for dye-sensitized solar cells: effect of auxiliary donor on optical and electrochemical properties. J Org Chem 2011;76:4910–20.

[47] Liang M, Wang Z-Y, Zhang L, Han H-Y, Sun Z, Xue S. New organic photosensitizers incorporating carbazole and dimethylarylamine moieties for dye-sensitized solar cells. Renew Energ 2011;36:2711–6.

[48] Ning Z, Zhang Q, Wu W, Pei H, Liu B, Tian H. Starburst triarylamine based dyes for efficient dye-sensitized solar cells. J Org Chem 2008;73:3791–7.

[49] Tian H, Yang X, Pan J, Chen R, Liu M, Zhang Q, et al. A triphenylamine dye model for the study of intramolecular energy transfer and charge transfer in dye-sensitized solar cells. Adv Funct Mater 2008;18:3461–8.

[50] Li G, Zhou Y-F, Cao X-B, Bao P, Jiang K-J, Lin Y, et al. Novel TPD-based organic D-[small pi]-A dyes for dye-sensitized solar cells. Chem Commun 2009;45:2201–3.

[51] Zhuang J, Su W, Li W, Zhou Y, Shen Q, Zhou M. Configuration effect of novel bipolar triazole/carbazole-based host materials on the performance of phosphorescent OLED devices. Org Electron 2012;13:2210–9.

[52] Agarwal N, Nayak PK, Ali F, Patankar MP, Narasimhan KL, Periasamy N. Tuning of HOMO levels of carbazole derivatives: new molecules for blue OLED. Synth Met 2011;161:466–73.

[53] Koumura N, Wang Z-S, Mori S, Miyashita M, Suzuki E, Hara K. Alkyl-functionalized organic dyes for efficient molecular photovoltaics [J Am Chem Soc 2006, 128, 14256–14257]. J Am Chem Soc 2008;130:4202–3.

[54] Ning Z, Tian H. Triarylamine: a promising core unit for efficient photovoltaic materials. Chem Commun 2009;45:5483–95.

[55] Yang C-H, Liao S-H, Sun Y-K, Chuang Y-Y, Wang T-L, Shieh Y-T, et al. Optimization of multiple electron donor and acceptor in carbazole-triphenylamine-based molecules for application of dye-sensitized solar cells. J Phys Chem C 2010;114:21786–94.

[56] Koumura N, Wang Z-S, Miyashita M, Uemura Y, Sekiguchi H, Cui Y, et al. Substituted carbazole dyes for efficient molecular photovoltaics: long electron lifetime and high open circuit voltage performance. J Mater Chem 2009;19:4829–36.

[57] Lin JT, Chen P-C, Yen Y-S, Hsu Y-C, Chou H-H, Yeh M-CP. Organic dyes containing furan moiety for high-performance dye-sensitized solar cells. Org Lett 2008;11:97–100.

[58] Kumchoo T, Promarak V, Sudyoadsuk T, Sukwattanasinitt M, Rashatasakhon P. Dipyrenylcarbazole derivatives for blue organic light-emitting diodes. Chem Asian J 2010;5:2162–7.

[59] Bonhôte P, Dias A-P, Papageorgiou N, Kalyanasundaram K, Grätzel M. Hydrophobic, highly conductive ambient-temperature molten salts. Inorg Chem 1996;35:1168–78.

[60] He J, Wu W, Hua J, Jiang Y, Qu S, Li J, et al. Bithiazole-bridged dyes for dye-sensitized solar cells with high open circuit voltage performance. J Mater Chem 2011;21:6054–62.

[61] Ito S, Murakami TN, Comte P, Liska P, Grätzel C, Nazeeruddin MK, et al. Fabrication of thin film dye sensitized solar cells with solar to electric power conversion efficiency over 10%. Thin Solid Films 2008;516:4613–9.

[62] Ning Z, Fu Y, Tian H. Improvement of dye-sensitized solar cells: what we know and what we need to know. Energ Environ Sci 2010;3:1170–81.

[63] Shen P, Liu X, Jiang S, Huang Y, Yi L, Zhao B, et al. Effects of aromatic π-conjugated bridges on optical and photovoltaic properties of N,N-diphenylhydrazone-based metal-free organic dyes. Org Electron 2011;12:1992–2002.

[64] Kinashi K, Lee K-P, Matsumoto S, Ishida K, Ueda Y. Alkyl substituent effects on J- or H-aggregate formation of bisazomethine dyes. Dyes Pigm 2012;92:783–8.

[65] Lin L-Y, Tsai C-H, Wong K-T, Huang T-W, Hsieh L, Liu S-H, et al. Organic dyes containing coplanar diphenyl-substituted dithienosilole core for efficient dye-sensitized solar cells. J Org Chem 2010;75:4778–85.

[66] Hagfeldt A, Graetzel M. Light-induced redox reactions in nanocrystalline systems. Chem Rev 1995;95:49–68.

[67] Teng C, Yang X, Yang C, Tian H, Li S, Wang X, et al. Influence of triple bonds as π-spacer units in metal-free organic dyes for dye-sensitized solar cells. J Phys Chem C 2010;114:11305–13.

[68] Qu S, Wang B, Guo F, Li J, Wu W, Kong C, et al. New diketo-pyrrolo-pyrrole (DPP) sensitizer containing a furan moiety for efficient and stable dye-sensitized solar cells. Dyes Pigm 2012;92:1384–93.

[69] Kim SH, Kim HW, Sakong C, Namgoong J, Park SW, Ko MJ, et al. Effect of five-membered heteroaromatic linkers to the performance of phenothiazine-based dye-sensitized solar cells. Org Lett 2011;13:5784–7.